OBSERVATIONS OF THE SOLAR WIND FROM CORONAL HOLES

M, NEUGEBAUER

Mail Stop 169-506

Jet Propulsion Laboratory, California Institute of Technology

Pasadena, CA 91109, USA

Abstract

The solar wind emanating from coronal holes (CH) constitutes a quasi-stationary flow whose properties change only slowly with the evolution of the hole itself. Some of the properties of the wind from coronal holes depend on whether the source is a large polar coronal hole or a small near-equatorial hole, The speed of polar CH flows is usually between 700 and 800 km/s, whereas the speed from the small equatorial CH flows is generally lower and can be <400 km/s. At 1 AU, the average particle and energy fluxes from polar CH are 2.5x108 $cm^{-2}sec^{-1}$ and 2,0 erg $cm^{-2}s^{-1}$. This particle flux is significantly less than the *4x108* $cm^{-2}sec^{-1}$ observed in the slow, interstream wind, but the energy fluxes are approximately the same. Both the particle and energy fluxes from small equatorial holes are somewhat smaller than the fluxes from the large polar coronal holes.

Many of the properties of the wind from coronal holes can be explained, at least qualitatively, as being the result of the effect of the large flux of outward-propagating Alfvén waves observed in CH flows. The different ion species have roughly equal thermal speeds which are also close to the Alfvén speed. The velocity of heavy ions exceeds the proton velocity by the Alfvén speed, as if the heavy ions were surfing on the waves carried by the proton fluid.

The elemental composition of the CH wind is less fractionated, having a smaller enhancement of elements with low first-ionization potentials than the interstream wind, the wind from coronal mass ejections, or solar energetic particles. There is also evidence of fine-structure in the ratio of the gas and magnetic pressures which maps back to a scale size of roughly 10 at the Sun, similar to some of the fine structures in coronal holes such as plumes, macrospicules, and the supergranulation.

1. Solar-wind speed

The solar wind emanating from polar coronal holes forms large, quasi-stationary high-speed streams. Figure 1 shows the velocity versus time profile for 16 encounters of the Ulysses spacecraft with the high-speed stream coming from the south polar coronal hole in 1992-1993. The plot starts just after the Ulysses gravity-assist at Jupiter, in February, 1992, when the spacecraft was 5.4 AU from the Sun at a heliographic latitude of -6.4° and extends to August, 1993, at distance of 4.3 AU and -38° latitude. During the first five months after the Jupiter flyby the velocity profile was rather complex with many low-speed streams typical of solar maximum conditions at that distance from the Sun. Then, as solar activity declined and Ulysses reached slightly higher southerly latitudes, the spacecraft started to detect the flow from the southern polar coronal hole; in the stream, the speed varied from 700 to 800 km/s, while between streams the speed declined to -400 km/s as the spacecraft entered the streamer belt and crossed the heliospheric current sheet. The highest-speed peak in the Figure was caused by a coronal mass ejection, probably associated with a class 3B solar flare on November 14. The quasi-periodicity of the pattern in Figure 1 matches the solar rotation rate as viewed from the orbit of Ulysses. After May, 1993, when its latitude was approximately -29°, the spacecraft was permanently above the latitude of the streamer belt (Bame et *al. 1993).* There was a further change in the profile in June, 1993, after which the spacecraft was perhaps always within the coronal hole flow.

Figure 1 illustrates what we have come to think of as a typical pattern of repeated encounters with streams from polar coronal holes, But the pattern is different at other phases of the solar cycle, Figure 2 shows the velocity profile obtained near Earth by the ISEE-3 spacecraft near solar maximum in 1978-9. The x's mark the periods of flow from five relatively small, near-equatorial coronal holes whose properties were analyzed by Neugebauer and Alexander (1991). There are perhaps another five coronal hole flows in that data set which were not selected for analysis. Note that the speeds of the selected

events never exceeded 700 km/s and were sometimes lower than 400 km/s. The point to be made is that the solar wind from small equatorial coronal holes (seCH) is usually quite different from the flow from the larger polar coronal holes (pCH); in this review the properties of the two types of coronal hole flows are summarized separately.

It was discovered by the Helios observations that the latitudinal edges of the high-speed streams from pCH are very sharp (Schwenn *et al.* 1978), with gradients of --100 km/sec/deg near 0.3 AU, and probably even steeper gradients closer to the Sun. The sharp edges are not apparent in the Ulysses data in Figure 1 because of interplanetary dispersion on the trailing edges (the fastest plasma runs away from the slower plasma immediately behind it) and because of the change in profile resulting from the shocks that form on the leading edges, The velocity gradients on the edges of streams from seCH have not been studied,

2. Average fluxes

Table I contrasts the fluxes of particles, energy, and the radial component of the magnetic field from pCH and from the slow solar wind between the fast pCH streams. Two sets of data have been used: IMP data taken at 1 AU between March, 1971 and July, 1974 (Feldman *et al,* 1977) and Helios data averaged between 0.3 and 1 AU between December, 1974 and May, 1976 (Marsch *et al.* 1984). These two non-overlapping sets of data were both obtained during periods when most of the high-speed streams could be associated with equatorward extensions of polar coronal holes. The sorting was done on the basis of solar wind speed, and so there may be a small amount of contamination of the "pCH" data with high speed streams caused by coronal mass ejections. The data were extrapolated to the solar surface by assuming radial flow -- i.e., an inverse square decrease of each parameter with distance from the Sun. There is, however, good evidence for greater-than-radial expansion in the corona; therefore each of the numbers in

the pCH column for the solar surface must be multiplied by an areal expansion factor, which is often modeled as being in the range of 5 to 10.

The data in Table I show that the particle flux is about a factor of 1,4- 1.8 lower and the density is about a factor of 3 lower in pCH flows than in the slow solar wind. The energy fluxes, which include the energy needed to overcome solar gravity, are roughly the same, however.

The particle and energy fluxes in our sample of five seCH were 2 x 10^8 $cm^{-2}s^{-1}$ and 1.2 erg $cm^{-2}s^{-1}$, which are slightly lower than the fluxes from the pCH. The average value of B_r in seCH has not been analyzed.

3. Internal State

Figure 3 (Neugebauer 1992) gives examples of proton and electron temperatures as a function of speed for different types of solar wind flow. In this figure, quasi-stationary flow is indicated by open symbols, while transient flow from coronal mass ejections is indicated by + and x. Coronal holes are shown by squares, with the pCH and seCH having velocities above and below 650 km/s, respectively. For all the quasi-stationary solar-wind flows, the proton temperature increases with the speed of the wind. This is in contrast to the case for transient flows, which are believed to be cooled by strong, 3-dimensional expansion en-route from the Sun to their point of observation at 1 AU. The bottom panel of Figure 3 shows, on the other hand, that the solar wind electron temperature is quite insensitive to the type of flow and that for pCH flows the electrons are substantially cooler than the protons. The electron temperature is determined principally by heat conduction from the corona, while the ion temperature is controlled by interplanetary processes, especially by waves. A simple-minded interpretation is that ion temperatures are determined by wave-particle interactions rather than by Coulomb collisions. Figure 4 gives some credence to that interpretation. It is a scatter diagram of the velocity dependence of the ratio of the proton thermal speed to the Alfvén speed

observed by Ulysses at the peaks and trailing edges of pCH flows. At the highest speeds, the ratio is close to 1. At lower speeds, the ratio is less than 1, probably due to a combination of cooling due to the expansion of the gas, increased Coulomb collisions in the slower, denser gas, and a decrease in the wave flux.

4. Waves

A large flux of Alfvén waves propagates away from the Sun through the solar wind (Belcher *et al. 1971).* Figure 5 shows an example of the importance of these waves in the pCH flows observed by Helios 2 between 0.29 and 0.54 AU, (Denskat *et al,* 1983). From top to bottom, this Figure shows: (1) The fluctuations in the magnitude of the magnetic field, normalized by the average field magnitude; this parameter is low for Alfvén waves. (2) The normalized fluctuations in one of the field components, which is large for a large flux of Alfvén waves. (3) The normalized fluctuations of plasma density, which are low for Alfvén waves. (4) The solar wind speed, which is highest in the pCH, as between April 13 and April 23. (5 to 7) The correlation between velocity and field for each of the three vector components, with the normalization and the sign of the field vector taken such that correlations of+ 1.0, 0, and -1.0 correspond to a pure flux of Alfvén waves propagating away from the Sun, to random fluctuations, and to an inward propagating wave flux, respectively. Correlations greater than +0.6 have been shaded. The relationship between high speeds, in this case associated with pCH flows, and strong fluxes of outward propagating Alfvén waves, often with $|\delta B|/B \approx 0.5$, is striking. Similar results are observed for seCH (Neugebauer 1992).

In his talk, Axford (these Proceedings) emphasized another indicator of the presence and importance of waves in the solar wind from coronal holes, namely the observation that the ratio of the temperatures perpendicular and parallel to the field $T_\perp/T_\parallel$ is > 1. Without the wave-particle interactions, the conservation of the magnetic moments of the ions would require $T_\perp/T_\parallel < 1$. These waves could be remnants of the wave field

responsible for the acceleration of the wind in coronal holes. Axford also suggested that these waves may be the low-frequency tail of the coronal wave spectrum which survives in the wind because it is less readily damped than the higher frequency part of the spectrum. But not all the waves originate at the Sun; additional waves must also be created in situ by the cyclotron instability of a $T_\perp/T_\parallel < 1$ configuration.

It was demonstrated in Figure 3 that for the flow from coronal holes the proton temperature is positively correlated with the solar wind speed and in Figure 4 that the proton thermal speed is close to the Alfvén speed= $B/\sqrt{(4\pi F/v)}$, where F is the ion flux and v is speed. It follows that the Alfvén speed should be correlated with the flow speed and that the flow speed should correlate inversely with f_{max}, the areal expansion factor of the streamlines or flux tubes between the photosphere and interplanetary space. Both those correlations are observed; the dependence of speed on f_{max} is discussed further in the paper by Wang in these Proceedings.

5. Minor Ions

The helium abundance in the solar wind is notoriously variable with the alpha particle density n_α ranging from nearly zero to almost half the density of protons n_p. CH flow is an exception, with n_α/n_p remaining quite steady at ≈ 0.048 in pCH. In seCH, n_α/n_p is also quite steady on the scale of minutes to hours, but its average value correlates with the average speed of the flow (Neugebauer 1992); i.e., n_α/n_p is lower in seCH than in pCH flows.

The abundances of elements heavier than helium also differ from one type of flow to another, although their variations are smaller than those observed for helium. For example, the Mg/O ratio observed over a 6-month period by the Solar Wind Ion Composition Spectrometer on Ulysses varied by more than an order of magnitude with a standard deviation of ≈40% [R. *von* Steiger, personal communication]. The variations are not random. Those ions with first ionization potentials (FIP) less than the energy of

Ly-α photons are over-abundant by factors up to ≈ 5 in the slow solar wind, in plasma from coronal mass ejections, and in gradual-event solar energetic particles. The abundances of these low-ionization-potential ions are, however, significantly less enhanced in the wind from coronal holes -- both pCH and seCH [R, von Steiger, G. Gloeckler, personal communication]. In other words, the FIP effect is much weaker for the flow from coronal holes than it is for the slow wind or the plasma confined to closed loops in the corona,

The charge-state of the ions heavier than helium is also different for coronal hole flows than for the slow or transient wind. The ionization temperature as determined, for example, by the ratio of O^{7+} to O^{6+} ion densities is lowest in coronal hole flows, higher in the slow solar wind, and highest of all in the plasma released in CMEs.

The distribution functions of the minor ions show the effect of the high wave flux in CH flows. In the wind from coronal holes, the different ion species have nearly equal thermal speeds rather than equal temperatures; i.e., their kinetic temperatures are proportional to their masses. In the pCH streams near 0.3 AU, Helios observed alpha-particle temperatures of-3 x 10^6 K, which is hotter than the corona (Marsch et *al.* 1982). And even at 1 AU the temperatures of some of the heavier ions, such as oxygen or iron, often exceed 10^7 K (Ogilvie et *al.* 1980)..

Another probable effect of the intense wave field is the differential streaming between the heavy ions and the protons in CH flows. Despite their greater mass and the greater amount of energy required to remove them from the solar gravitational field, the alphas stream away from the Sun faster than the protons. Figure 6 (Feldman *et al.* 1993) shows two one-dimensional ion spectra of the high-speed wind from a coronal hole. The plots show counts versus energy per unit charge, converted to units of $v\sqrt{(M/Q)}$, with protons and alpha-particles constituting the peaks at the lower and higher values of $v\sqrt{(M/Q)}$, respectively. Above the left-most peak with $v = V_1$ is a secondary proton peak close to $V_1 + V_A$, where V_A is the Alfvén speed. The alpha-particle peak is at $V_1 + V_A$,

rather than at V_1, which would be the case if the two ion species had the same flow speed. A simple view is that the alphas are surfing through the proton sea on the crests of the outward propagating Alfvén waves, but a detailed theory has not yet been developed to explain quantitatively why this happens (Isenberg 1984). Feldman et al. (1993) have interpreted this phenomenon as evidence that there are two sources of the solar wind in coronal holes: (1) a thermally driven, low-speed wind whose flux is so low that it cannot drag alpha-particles out into the wind and (2) fast, helium-rich plasma jets, driven by reconnection, which interact with and accelerate the low-speed, helium poor wind to high speed. In that scenario, the jets would also be the principal source of the waves observed in CH flows.

It is interesting to note that the Alfvén speed V_A decreases rapidly with solar distance. If the data from Helios and other spacecraft (e.g., Figure 6) are extrapolated inward, say to the solar-wind critical point, the energy lost by the alpha-particles $\Delta(m_\alpha V_A^2/2)$ is so large that it must bean important source of energy for accelerating the wind from coronal holes.

6. Small-Scale Structures

At distances from the Sun of 1 AU or greater, one of the distinguishing features of CH flow is the relative constancy of all parameters other than the directions of v and B, which are affected by the waves; i.e., the density, field magnitude, ion and electron temperatures, and n_α/n_p do not fluctuate very much. But it was possible to find some fine structure in the Helios data inside 1 AU. Figure 7, from a paper by Thieme et al. (1990), shows time profiles of VW = proton speed after subtraction of fluctuations due toAlfvén waves, v_α = alpha-particle speed, P_{gas} = gas pressure, P_{mag} = magnetic pressure, P_{tot} = total pressure = pgas + P_{mag}, and the plasma β. These data were obtained by Helios 1 in 1975 at a solar distance of 0.66 to 0.60 AU. The vertical dotted lines mark occasions of pronounced anticorrelation between the gas and magnetic pressures, even though the total

pressure remains very constant, At the closest distances to the Sun, 0.3 to 0.5 AU, the sizes of the blobs of extremes of gas or magnetic pressures correspond to angular dimensions on the Sun between 1 and 2°. Thieme et al. suggest that these structures are remnants of fine structures in coronal holes, such as plumes and macrospicules which are connected to the chromospheric network.

7. Summary

Table II summarizes the properties of pCH and seCH discussed above. An asterisk on the right denotes a property that indicates the presence or effect of a large flux of outward propagating Alfvén waves in the flow from coronal holes. An outstanding question for future research is the relationship between and the relative roles of waves versus jets in heating the corona and accelerating the wind in coronal holes.

References

Bame, S. J., Goldstein, B. E., Gosling, J. T., *et al.:* 1993, *Geophys. Res. Lett.* Submitted,

Belcher, J. W., Davis, L., Jr.: 1971, *J. Geophys. Res.* 76,3534-3563

Denskat, K. U., Neubauer, F. M.: 1983, in *Solar Wind Five,* M. Neugebauer (Ed.), NASA, Washington, p. 81-91

Feldman, W. C., Asbridge, J. R., Bame, S. J., *et al.*: 1977, in *The Solar Output and its Variation, O.* R, White (Ed.), Colorado Assoc. Univ. Press, Boulder, p, 351-382

Feldman, W, C., Gosling, J. T., McComas, D. J., *et al.*: 1993, *J. Geophys. Res* 98,5593

Isenberg, P. A.: 1984, *J. Geophys. Res.* 89,6613

Marsch, E., Mühlhaüser, K.-H., Rosenbauer, H., *et al.:* 1982, *J, Geophys. Res.* 87,35

Marsch, E., Richter, A. K.: 1984, *J. Geophys. Res.* 89,6599

Neugebauer, M.: 1992, in *Solar Wind Seven,* E, Marsch, R. Schwenn (Ed.), Pergamon Press, Oxford, p. 69-78

Neugebauer, M., Alexander, C. J.: 1991, *J. Geophys. Res.* 96,9409

Ogilvie, K. W., Bochsler, P., Coplan, M. A., et *al.:* 1980, *J. Geophys. Res.* 85,6069

Schwenn, R., Montgomery, M. D., Rosenbauer, H., *et al.:* 1978, *J. Geophys. Res. 83,* 1o11

Thieme, K. M., Marsch, E., Schwenn, R.: 1990, *Arm Geophys.8,713*

Table I. Typical fluxes in solar-wind streams from polar coronal holes and from the slow solar wind

		At 1 AU		At the Sun	
		Polar co on holes	**Slow wind**	**Polar coronal holes**	**Slow wind**
nv, cm^{-2} s^{-1}	Helios	$2.2 \pm 1.1 \times 10^{8}$	$4.0 \pm 0.8 \times 10^{8}$	1.0×10^{13}	1.8×10^{13}
	IMP	$2.7 \pm 0.4 \times 10^{8}$	$3.9 \pm 1.5 \times 10^{8}$	1.2×10^{13}	1.8×10^{13}
Energy, erg $cm^{-2}s^{-1}$	Helios	1.6 ± 0.4	1.7 ± 0.7	0.7×10^{5}	0.8×10^{5}
	IMP	2.2 ± 0.4	1.7 ± 0.6	1.0×10^{5}	0.8×10^{5}
B_r, G	Helios	$3.2 \pm 1.5 \times 10^{-5}$	$2.9 \pm 1.9 \times 10^{-5}$	.5	1.3

Table II. Summary of the properties of the solar wind flowing from large polar coronal holes (pCH) and from small, equatorial coronal holes (seCH)

Parameter	pCH	seCH	
V, km/s	750-800	Can be <400	
nV, 108 $cm^{-2}s^{-1}$	2.5	2,0	
Energy flux, erg $cm^{-2}s^{-1}$	2,0	1.7	
Proton, electron temperatures	$T_p > T_e$	T_p can be $< T_e$	*
$V_{thermal,\ p}/V_A$	≈1	Can bee 1	*
Waves	Strong flux of outward propagating Alfvén waves	Strong flux of outward propagating Alfvén waves	*
n_α/n_p	≈0.048	s0.048 Increases with V	
FIP effect	Small	Small	
$v_\alpha - v_p$	$\approx V_A$	?	*
Heavy ion temperature	$T_i \sim m_i$	$T_i \sim m_i$	*
Fine structure	Supergranule scales	?	

FIGURE CAPTIONS

Fig. 1. Hourly averages of the solar wind speed as observed by the solar wind plasma experiment on Ulysses from February, 1992 to August, 1993 (Bame et al. 1993).

Fig. 2. Hourly averages of the solar wind speed as observed near Earth by the solar wind plasma experiment on ISEE 3 from August, 1978 to August, 1979.

Fig, 3. Proton (top) and electron(bottom) temperatures versus solar-wind speed averaged over intervals of different types of flow (Neugebauer 1992), Open symbols denote quasi-stationary wind while + and x refer to coronal mass ejections. The notation is CH = coronal holes, IS = interstream plasma, PS = the high-density plasma sheet in which the heliospheric current sheet is embedded, HAE = helium abundance enhancements, and BES = hi-directional electron streaming.

Fig. 4. Scatter plot of hourly averages of the ratio of the proton thermal speed to the Alfvén speed versus the flow speed of the wind as observed at the peaks and trailing edges of polar coronal hole streams observed by Ulysses.

Fig. 5. Plots of various parameters indicative of the presence of Alfvén waves as observed by Helios 2 (Denskat and Neubauer 1983), See the text for further explanation.

Fig. 6. Solar-wind ion spectra measured in plasma from a polar coronal hole observed by IMP (Feldman, et al. 1993).

Fig 7. Time profiles of various plasma parameters observed by Helios (Thieme et al. 1990). Further explanation is given in the text, Pressures are given in units of C* = 10^{-10} dyne cm^{-2}.

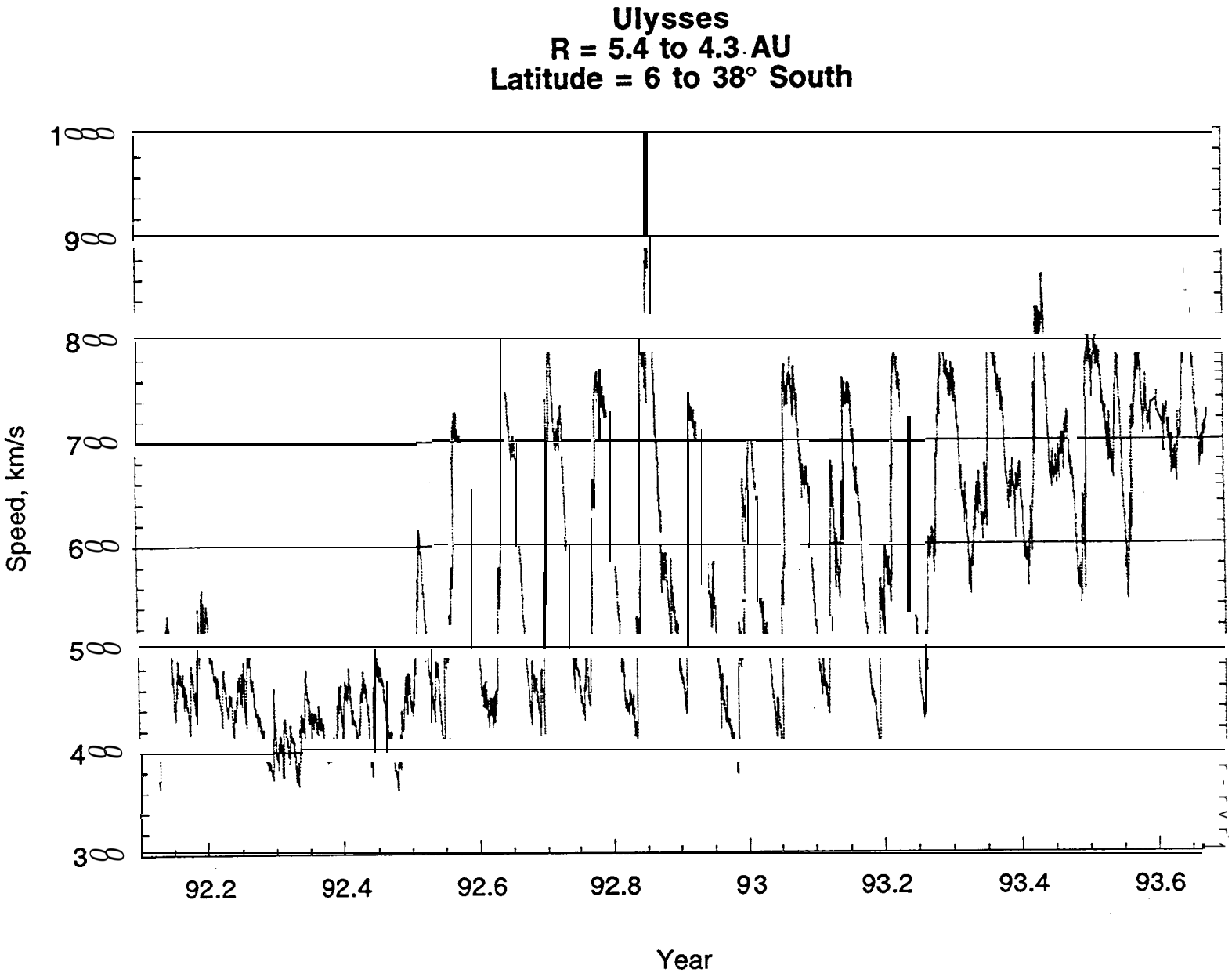
Ulysses
R = 5.4 to 4.3 AU
Latitude = 6 to 38° South
Speed, km/s
100
90
80
70
60
50
40
30
92.2
92.4
92.6
92.8
93
93.2
93.4
93.6
Year

Fig. 1

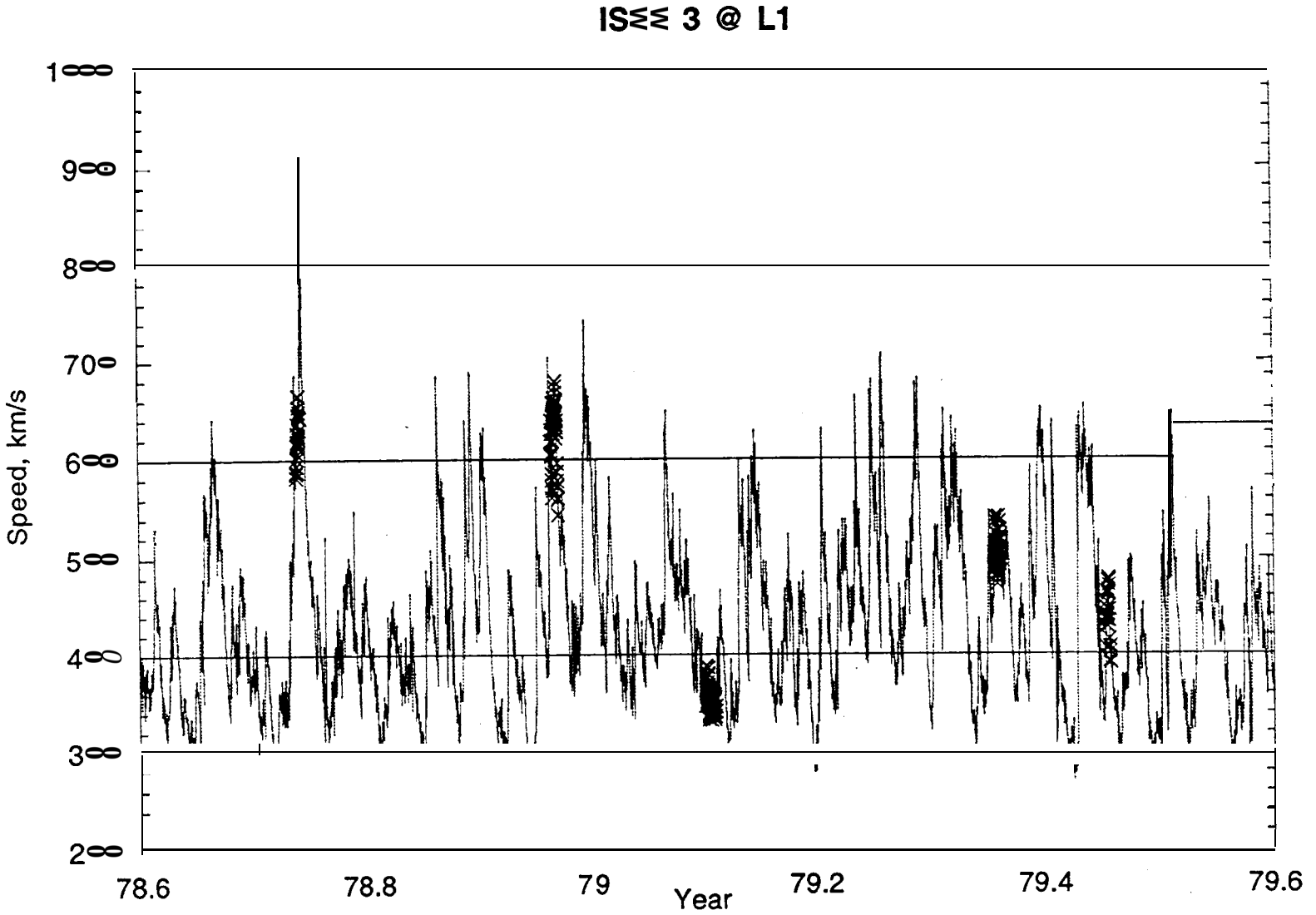
ISEE 3 @ L1
Speed, km/s
1000
900
800
700
600
500
400
300
200
78.6
78.8
79
79.2
79.4
79.6
Year

Fig. 2

Ulysses
Non-Interaction Regions
1992.5 - 1993.4
5.33-4.77 AU
13.4-29.7° South

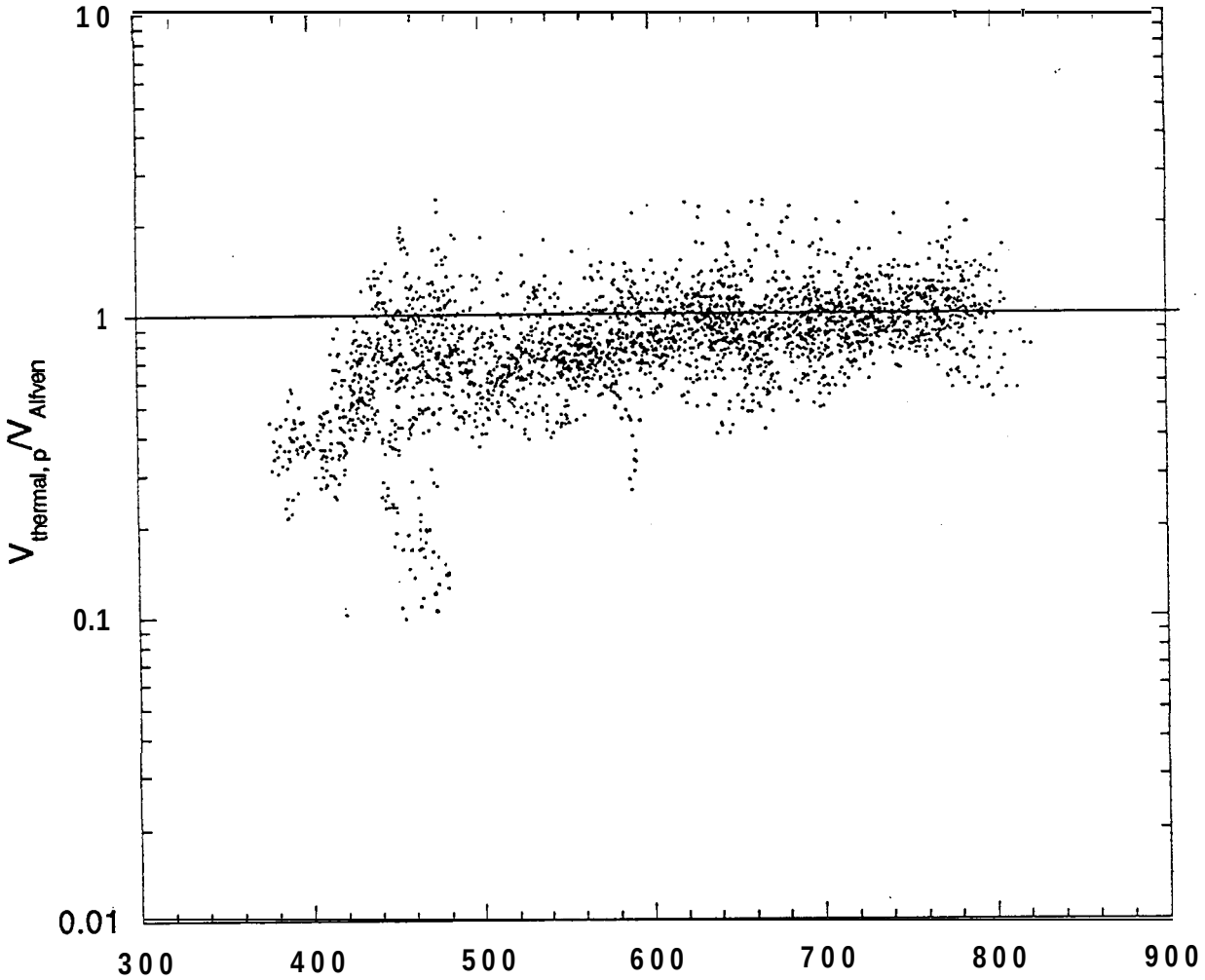

Fig 4

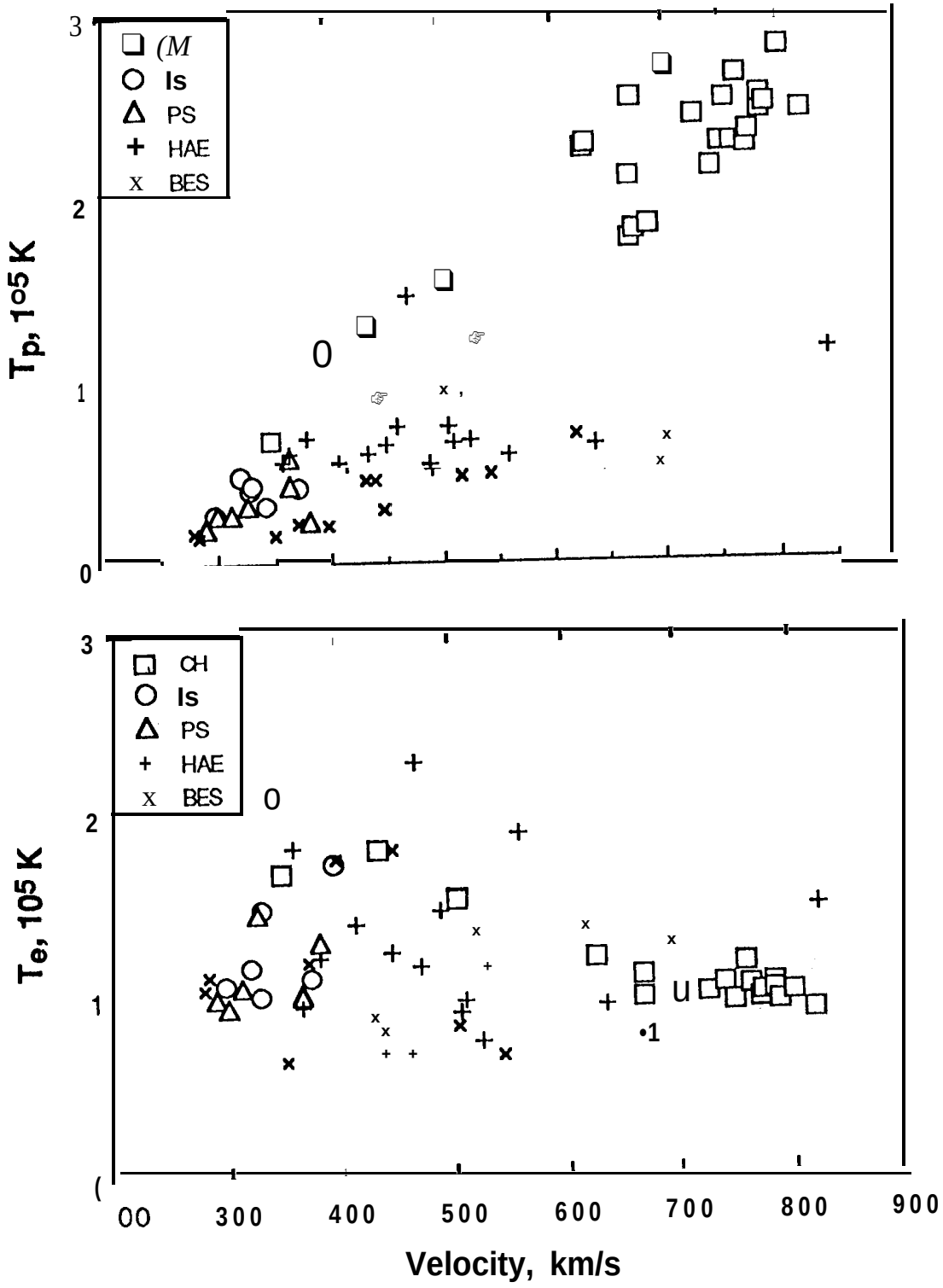
(M
Is
PS
HAE
BES
Tp, 10^5 K
CH
Is
PS
HAE
BES
Te, 10^5 K
300
400
500
600
700
800
900
Velocity, km/s

Fig 3

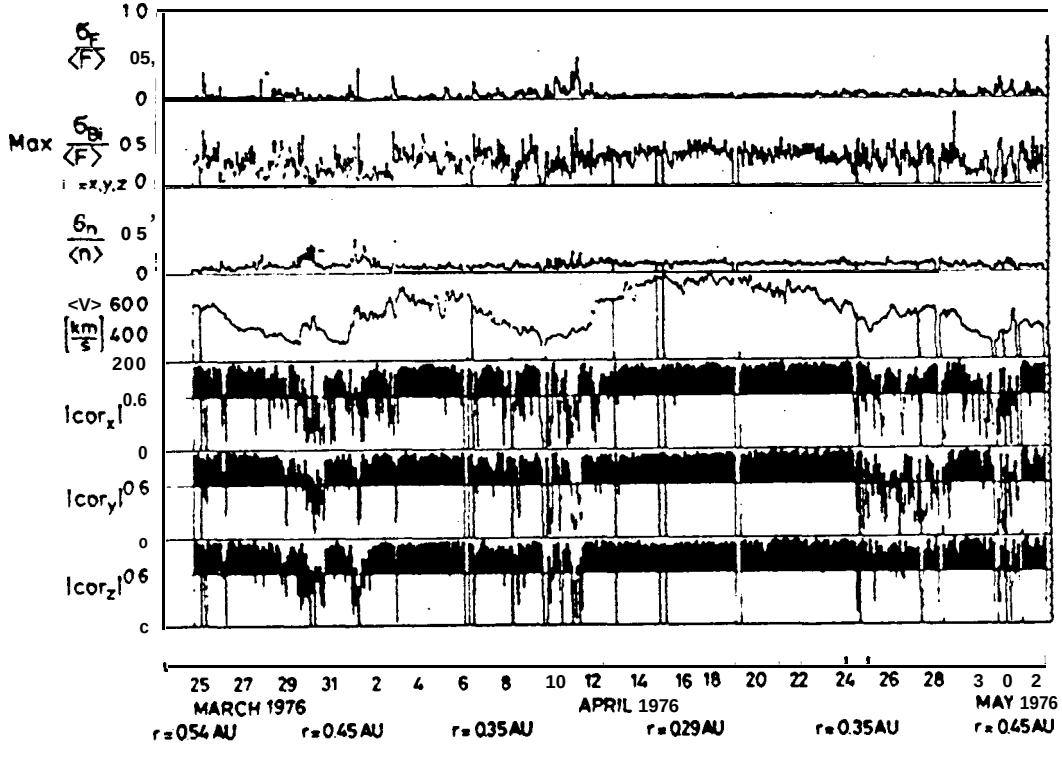
1.0
$\frac{\sigma_F}{\langle F \rangle}$
0.5
0
Max $\frac{\sigma_{Bi}}{\langle F \rangle}$
0.5
i = x,y,z
0
$\frac{\sigma_n}{\langle n \rangle}$
0.5
0
<V>
600
$\left[\frac{km}{s}\right]$
400
200
$|cor_x|$
0.6
0
$|cor_y|$
0.6
0
$|cor_z|$
0.6
0
25 27 29 31 2 4 6 8 10 12 14 16 18 20 22 24 26 28 30 2
MARCH 1976
APRIL 1976
MAY 1976
r = 0.54 AU
r = 0.45 AU
r = 0.35 AU
r = 0.29 AU
r = 0.35 AU
r = 0.45 AU

fig. 5

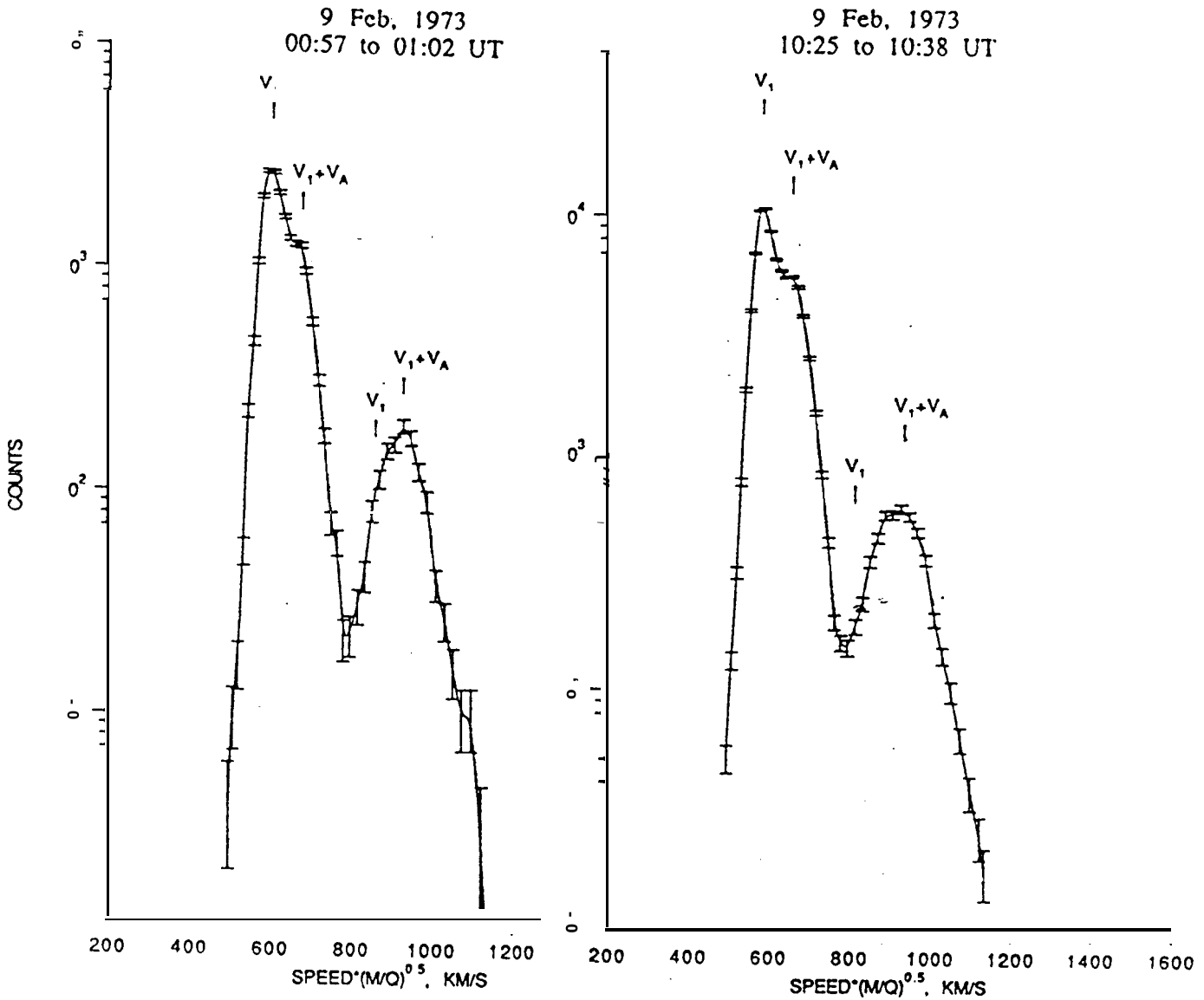
9 Feb, 1973
00:57 to 01:02 UT
9 Feb, 1973
10:25 to 10:38 UT
COUNTS
V_1
V_1+V_A
V_1
V_1+V_A
V_1
V_1+V_A
V_1
V_1+V_A
200
400
600
800
1000
1200
1400
1600
SPEED*(M/Q)$^{0.5}$, KM/S
SPEED*(M/Q)$^{0.5}$, KM/S

Fig 6

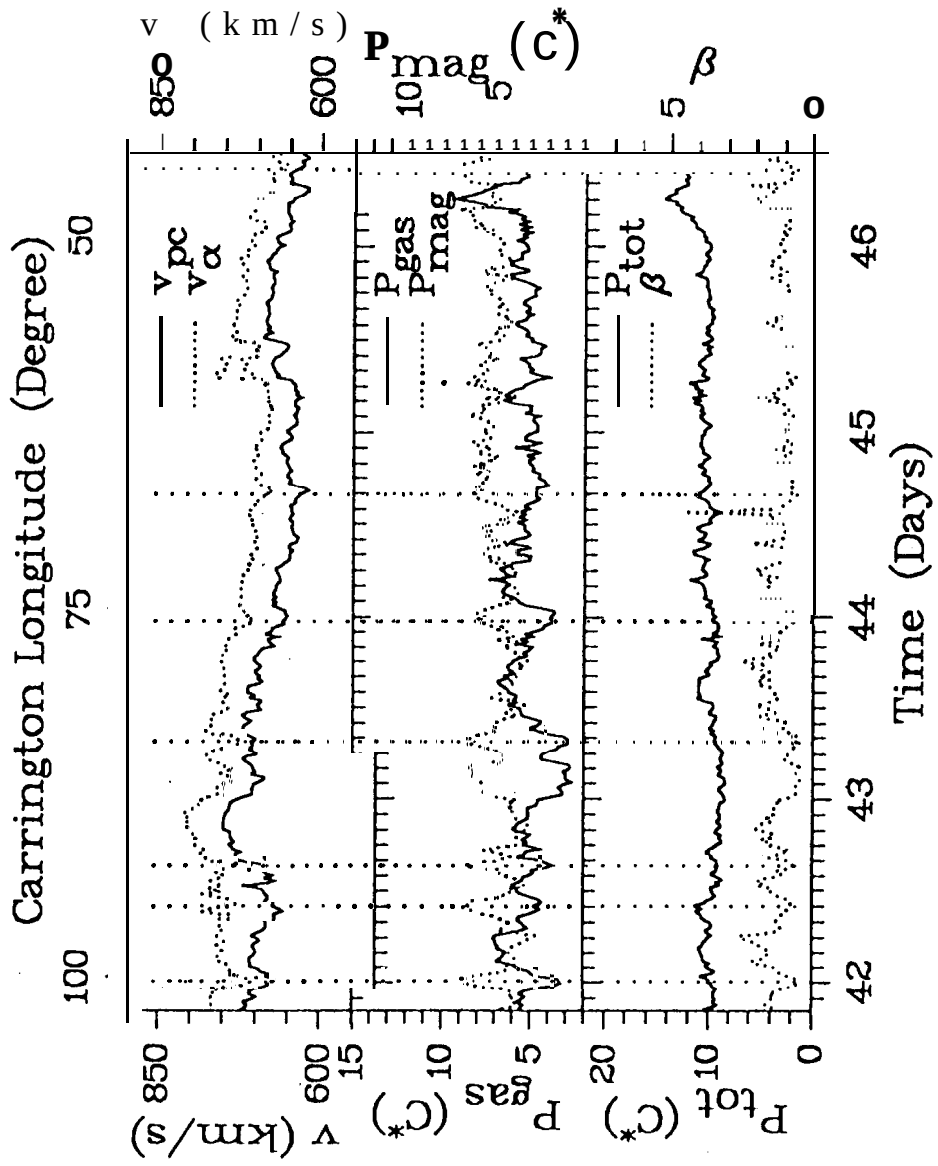
v (km/s)
850
600
15
10
5
20
10
0
100
75
50
42
43
44
45
46
Carrington Longitude (Degree)
Time (Days)
v_{pc}
v_{α}
P_{gas}
P_{mag}
P_{tot}
β
P_{mag} (C*)
P_{gas} (C*)
P_{tot} (C*)
v (km/s)
β

Fig 7